17th World Conference on Earthquake Engineering, 17WCEE
Sendai, Japan - September 13th to 18th 2020
Submission N°: C-001607
Registration N°: S-A01280

STOCHASTIC SETTLEMENT AND TILT TIME HISTORIES FOR DYNAMIC ANALYSIS OF STRUCTURES ON LIQUEFIABLE GROUND

Z. Bullock[(1)], S. Dashti[(2)], A. B. Liel[(3)], K. A. Porter[(4)]

[(1)] *PhD Candidate, University of Colorado Boulder, zachary.bullock@colorado.edu*
[(2)] *Associate Professor, University of Colorado Boulder, shideh.dashti@colorado.edu*
[(3)] *Associate Professor, University of Colorado Boulder, abbie.liel@colorado.edu*
[(4)] *Research Professor, University of Colorado Boulder, keith.porter@colorado.edu*

Abstract

Performance-based procedures for estimating the liquefaction-induced settlement and tilt of structures on shallow foundations have recently been produced by the authors. These procedures can be combined with traditional structural analysis to develop holistic estimates of the foundation and superstructure damage in an earthquake. However, analysis of the interaction of the foundation and superstructure has been limited to the application of the permanent values of settlement and tilt to the foundation. The results of structural analysis may be sensitive not only to the settlement and tilt of the foundation after shaking, but also to their time histories during shaking. This study develops methodologies for generating stochastic time histories of settlement and tilt based on estimates of average settlement, residual tilt, and peak transient tilt that can be obtained from existing models, while also incorporating information regarding the transverse acceleration time history. Using the procedures outlined in this paper, one can inject foundation's settlement and tilt time histories into the nonlinear dynamic structural analysis stage of second-generation performance-based earthquake engineering, such as in FEMA P-58, a new capability. The development includes the following elements. First, general functional forms for the time histories of the accumulation of Arias intensity, cumulative absolute velocity, foundation settlement, and foundation tilt are developed. Then, parameters for use in these functions are obtained using data from centrifuge testing of shallow-founded structures on liquefiable ground. Finally, results from structural analyses with and without consideration of the time histories of settlement and tilt are presented and the influence of their inclusion is demonstrated. The example analyzed in this study shows that the inclusion of transient foundation displacements can result in larger demands in the superstructure compared to neglecting foundation displacements or applying them pseudostatically after dynamic analysis. These results highlight the importance of considering transient foundation displacements when analyzing structures above liquefiable ground and the need for methodologies for obtaining time histories of foundation settlement and tilt.

Keywords: liquefaction; shallow foundations; foundation settlement; foundation tilt; dynamic analysis

1. Introduction

Recent studies have produced probabilistic procedures for estimating the permanent settlement [1,2] and residual and peak transient tilt [3] of shallow-founded structures above liquefiable ground. Although such procedures provide insight into the final state of a shallow-founded structure and the peak rocking response during shaking, they do not allow structural engineers to incorporate settlement and tilt into dynamic time history analysis of structures. Indeed, applying foundation's settlement and tilt to a structure pseudostatically after shaking may allow structural engineers to partially account for their influence on structural response, but the peak response of the superstructure (e.g., peak interstory drifts) may be affected by the interaction of the transient rocking response and the horizontal acceleration. Incorporating this interaction into dynamic structural analysis requires either development of a model that accounts for soil-structure-interaction (SSI), or time histories of the foundation settlement and tilt, which can be used to simulate a foundation's rocking response during shaking. The approach accounting for SSI has limitations that may render it impractical for many applications. Specifically, no spring models that include the effects of liquefaction have been developed. Additionally, analyses including the full soil column are much more computationally expensive than analyses of the superstructure in isolation.

This paper presents methodologies for obtaining time histories of the settlement and tilt of shallow-founded structures on liquefiable ground. The time histories are derived from estimates of permanent settlement, residual tilt, and peak transient tilt, as well as properties of an associated (input) acceleration time history. Data from centrifuge experiments are used to develop and validate the functions. Sets of time histories (i.e., acceleration, settlement, and tilt) corresponding to a certain input ground motion enable structural engineers to account for liquefaction in dynamic structural analysis – without developing a full, 3-D model of the soil column and modeling the soil-foundation interface – for the first time. Finally, time histories generated using the proposed methodology are used to perform dynamic time history analysis of a structure, and the results are compared to both the fixed-base case with horizontal acceleration only applied as well as the fixed-base case with pseudostatic foundation settlement and tilt applied following shaking. The initial findings suggest that the transient settlement and tilt have a significant effect on peak transient and residual drifts in the superstructure, indicating that neglecting them or applying them pseudostatically may be inaccurate and unconservative.

2. Time History Functional Forms

This section presents the functional forms used for the time histories of foundation settlement and tilt. The functional forms are designed (i) to maximize their ability to fit observed time histories from centrifuge test results [4-7], as discussed subsequently; (ii) to make use of parameters that have clear physical interpretations; and (iii) to simplify implementation.

2.1 Settlement time histories

Eq. (1) gives the functional form used for time histories of foundation settlement. In this equation, t is time in sec, $S(t)$ is the settlement at time t in mm, t_o is the time of the onset of accumulation in sec, D_a is the duration of accumulation in sec, n is a unitless shape parameter, and S is the permanent settlement after shaking in mm. Note that $H(\cdot)$ is the Heaviside step function of the argument.

$$S(t) = H(t - t_o)[1 - \exp(-3\,(t - t_o)^n / D_a^n)]S \tag{1}$$

This functional form is adapted from the exponential model commonly used in variogram analysis [8] because it shares some characteristics that are important in this application (i.e., that the function gives a positive value for $t \geq 0$ and monotonically approaches S for large t). This functional form assumes that settlement increases monotonically over the course of shaking. The coefficient of 3 in Eq. (1) results in the duration of accumulation (D_a) corresponding to the time needed to accumulate 95% of the final settlement. The selection of this coefficient is arbitrary, but selecting 3 (and accepting that D_a corresponds to accumulation of 95% of the final

settlement) is convenient for interpretation of D_a and for clarity in Eq. (1). Figure 1 shows an example of a settlement time history that demonstrates the physical interpretation of t_o and D_a as well as the influence of n. Note that t_o is the time at which settlement begins to accumulate – it is not tied to any other phenomenological definition of liquefaction.

2.2 Tilt time histories

Unlike settlement, we do not assume that tilt increases monotonically, but rather expect it to both oscillate cyclically and accumulate during shaking; as a result, the functional form for tilt is more complex. Eq. (2) provides the functional form for tilt, where $\theta(t)$ is the tilt at time t in degrees, $\theta_m(t)$ is the monotonic component of tilt at time t in degrees, and $\theta_t(t)$ is the transient component of tilt at time t in degrees. $\theta_m(t)$ reflects our expectation that tilt will, in general, accumulate over the course of shaking and arrive at some final value (called the residual tilt). $\theta_t(t)$ reflects our expectation that tilt will also involve a cyclic component and allows for a value of peak transient tilt that exceeds the residual tilt.

$$\theta(t) = \theta_m(t) + \theta_t(t) \tag{2}$$

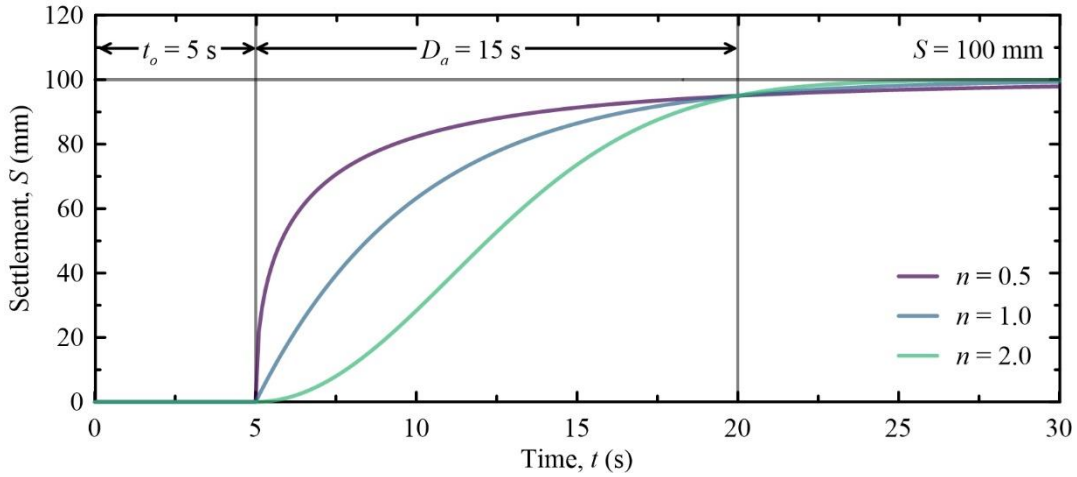

Fig. 1 – Influence of the settlement time history parameters (t_o, D_a, and n) in Eq. (1) on the shape of the resulting time history. This example uses $t_o = 5$ s, $D_a = 15$ s, n between 0.5 and 2.0, and $S = 100$ mm.

Eq. (3) gives the functional form for the monotonic component of tilt, where θ_r is the residual tilt after shaking in degrees. This function uses the same form as the one used for settlement in Eq. (1). Eq.(4) gives the functional form for the transient component of tilt, where $\bar{W}_1(\cdot)$ and $W_2(\cdot)$ are windowed noise functions given by Eqs. (9) and (10) and θ_{pt} is the peak transient tilt in degrees. Eq. (5) defines the envelope for the windowed noise in Eq. (4) in the form of the probability density function (PDF) of a Gumbel distribution [9]. Figure 2 shows time histories of θ_m, θ_t, $\bar{W}_1$, W_2 and θ to demonstrate how they reflect the relevant parameters from the acceleration time history (t_{PGA} and $T_{1,ff}$). Note that the time of onset, the duration of accumulation, and the shape parameter (t_o, D_a, and n) can be interpreted similarly as in Figure 1.

$$\theta_m(t) = H(t - t_o)[1 - \exp(-3\,(t - t_o)^n / D_a^n)]\theta_r \tag{3}$$

$$\theta_t(t) = H(t - t_o)\bar{W}_1(t - t_o)W_2(t - t_o)\left(\theta_{pt} - \theta_b(t)\right) \tag{4}$$

$$W_1(t - t_o) = (1/\beta)\exp[-(z + \exp(-z))] \tag{5}$$

Eqs. (6), (7), and (8) define the parameters in the Gumbel PDF in Eq. (5), where t_{PGA} is the time at which the peak ground acceleration occurs in the associated acceleration time history in sec. These parameters ensure that (i) the maximum amplitude of the noise occurs at precisely t_{PGA}; (ii) the cyclic noise is zero before

the onset of shaking; (iii) the final tilt time history does not include any physically unjustifiable discontinuities that may prevent their use in numerical time history analysis; and (iv) that the cyclic noise is nearly zero after time equal to D_a has passed after onset. The use of t_{PGA} in this context will be discussed in a subsequent section. Finally, the envelope is normalized according to Eq. (9) before being used in Eq. (4), such that the maximum value of the envelope is equal to 1.

$$\mu = t_{PGA} \tag{6}$$

$$\beta = D_a/2\pi \tag{7}$$

$$z = (t - \mu)/\beta \tag{8}$$

$$\bar{W}_1(t - t_o) = W_1(t - t_o)/W_1\,(t_{PGA} - t_o) \tag{9}$$

Eq. (10) defines the cyclic amplitude of the windowed noise in Eq. (4), where $T_{1,ff}$ is the predominant period of the associated acceleration time history in sec. The use of $T_{1,ff}$ in this context will also be discussed in a subsequent section. This functional form for $W_2(t)$ ensures that the maximum value of the transient component of tilt occurs at exactly t_{PGA} and that the maximum value of the total tilt is exactly equal to θ_{pt}.

$$W_2(t - t_o) = \cos\left(2\pi/T_{1,ff}\,(t - t_{PGA})\right) \tag{10}$$

3. Time History Parameters

This section provides guidance regarding the determination of the parameters needed for Eqs. (1) through (10) and validation of assumptions used in their development.

3.1 Database

Table 1 summarizes the database of centrifuge results used to develop parameters for the settlement and tilt time histories. The structure was situated on a mat foundation and the liquefiable soil was fully saturated for each test. The centrifuge prototype structures included variation in foundation width, structure height, structure period, and number of stories (i.e., number of degrees of freedom). The specimens were subjected to ground motions in flight that included variation in intensity and frequency content.

3.2 Determination of parameters in the settlement functional form

The functional form for settlement described by Eq. (1) has three parameters: the time of onset (t_o), the duration of accumulation (D_a), and the shape parameter (n). In this section, we use nonlinear regression to determine these three parameters for both the settlement time histories and plots of the accumulation of Arias intensity (i.e., the Husid plot [10]) or cumulative absolute velocity with time. Eq. (11) defines the Arias intensity [11] at time t and Eq. (12) defines the cumulative absolute velocity at time t. These functions are used because we expect the accumulation of Arias intensity or cumulative absolute velocity (i.e., the accumulation of energy applied to the system) over the course of shaking to correspond to the foundation settlement. Eq. (13) shows the function used to determine the three parameters by nonlinear regression, where $Y(t)$ is $I_A(t)$ or $CAV(t)$, $a(t)$ is the acceleration at time t, and Y is I_A or CAV for the acceleration time history. We report $a(t)$ in units of cm/s^2 and I_A and CAV in units of cm/s.

$$I_A(t) = \pi/2g \int_0^t a(t)^2 dt \tag{11}$$

$$CAV(t) = \int_0^t |a(t)| dt \tag{12}$$

$$Y(t) = H(t - t_o)[1 - \exp(-3\,(t - t_o)^n/D_a^n)]Y \tag{13}$$

Figure 3 provides an example of an acceleration time history and the associated Husid plot for I_A, including the fitted curve obtained using Eq. (13). The quality of the fit demonstrated in Figure 3(b) is consistent for the plots of the accumulation of both I_A and CAV and the settlement time histories for all of the tests in Table 1 ($R^2 > 0.95$).

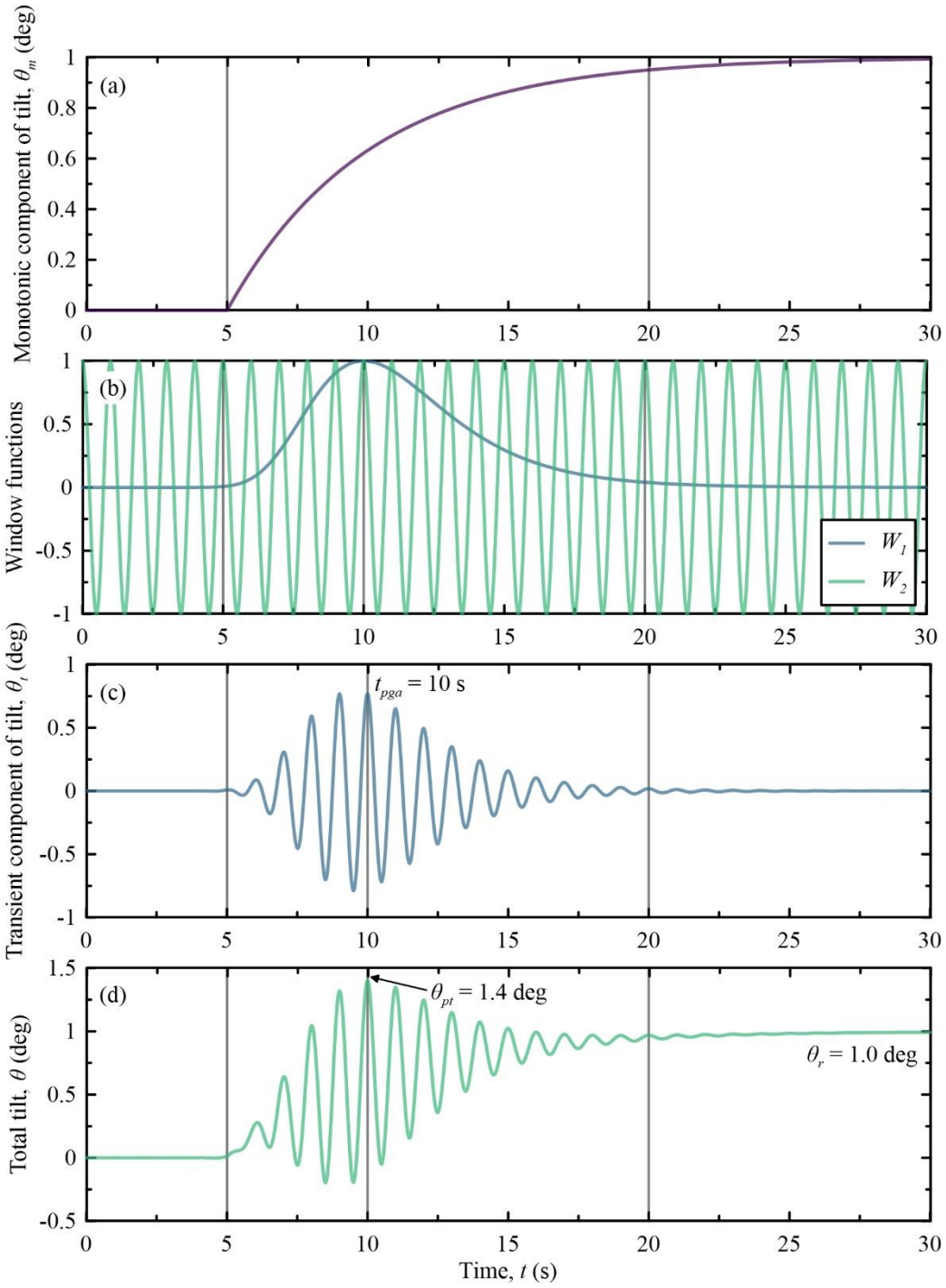

Fig. 2 – Influence of the tilt time history parameters on the shape of the time history given by Eq. (2) through Eq. (10). This example uses $t_o = 5$ s, $D_a = 15$ s, $n = 1.0$, $t_{pga} = 10$ s, $T_{1,ff} = 1.0$ s, $\theta_r = 1.0$ deg, and $\theta_{pt} = 1.4$ deg.

Figure 4 shows the correlations between parameters determined for each centrifuge test result for Arias intensity, cumulative absolute velocity, and settlement. Generally, the time of onset (t_o), duration of accumulation (D_a), and shape parameter (n) for the settlement of the structure in the centrifuge test agrees better with the values for CAV recorded in the far field than those for I_A. I_A also displays some systematic bias (e.g., D_a for I_A is systematically smaller than D_a for S, and n for I_A is substantially larger than n for S for three cases). These results suggest that the time history of settlement has approximately the same shape as the plot of the accumulation of CAV. Note that CAV has previously been identified as the most efficient predictor of foundation settlement [2, 12, 13]. Because this study uses a relatively small sample size, additional numerical or experimental research is needed to validate this finding, or to develop a more sophisticated model for identifying these parameters for the settlement time history.

Table 1 – Centrifuge test results used in this study.

Source	Number of tests
Dashti et al. [4,5]	18
Olarte et al. [6]	10
Paramasivam et al. [7]	3

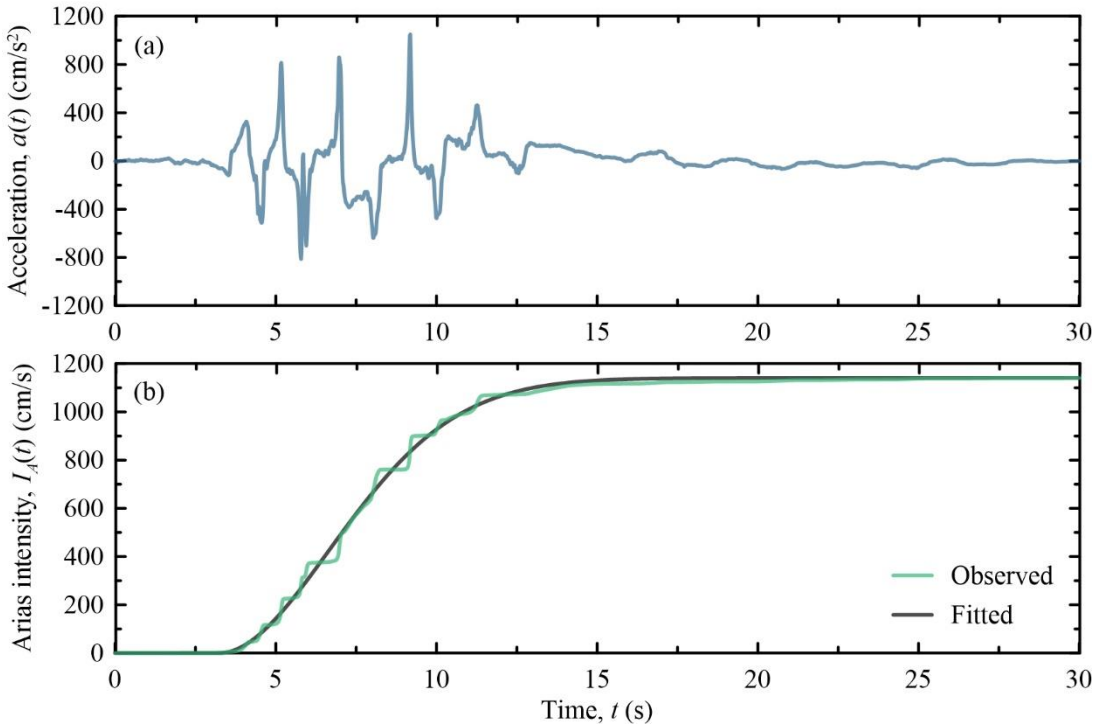

Fig. 3 – Examples of (a) an acceleration time history and (b) the associated Husid plot for Arias intensity. The fitted model of the Husid plot uses $t_o = 3.26$ s, $D_a = 9.21$ s, and $n = 1.864$.

3.2 Determination of parameters in the tilt functional form

The functional forms for the tilt time histories described in Eqs. (2) through (10) assume (i) that the peak transient tilt occurs at the same time as the PGA of the input acceleration time history; and (ii) that the cyclic portion of the tilt has a single frequency corresponding to the predominant period of the input acceleration time history. This section verifies these assumptions.

Figure 5(a) shows the relationships between the time of the peak ground acceleration (t_{PGA}) and the time of the peak ground velocity (t_{PGV}) and the time of the peak transient tilt (t_θ) for the centrifuge results

summarized in Table 1. The correlation between t_θ and t_{PGA} is stronger than that between t_θ and t_{PGV} (with the exception of a single outlier), which supports the use of t_{PGA} in Eqs. (6) and (9). Note that there are three cases where t_{PGV} is significantly larger than t_θ. Figure 5(b) provides similar information regarding the relationships between the predominant period of the tilt time histories recorded in the tests (T_θ) and the predominant period of the far field ground acceleration ($T_{1,ff}$) and the structure period (T_{st}). T_θ is closely related to $T_{1,ff}$, but not T_{st}. Again, there is a single outlier. We recommend the use of $T_{1,ff}$ in Eq. (10).

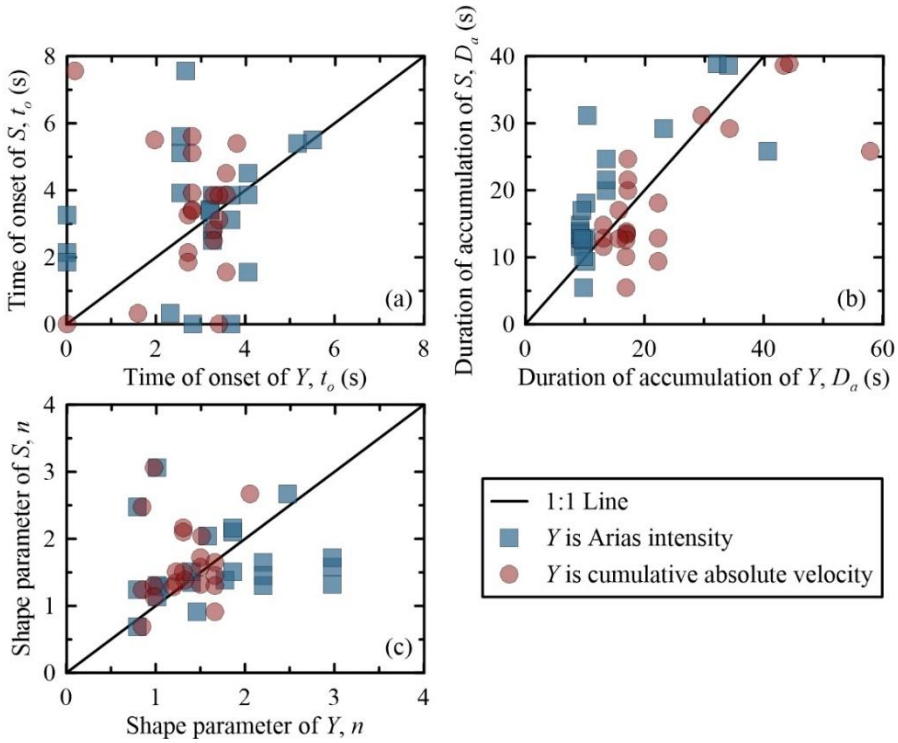

Fig. 4 – Relationships among fitted values of (a) the time of onset, (b) the duration of accumulation, and (c) the shape parameter for the plots of the accumulation of Arias intensity and cumulative absolute velocity and those of the settlement time histories measured in the centrifuge.

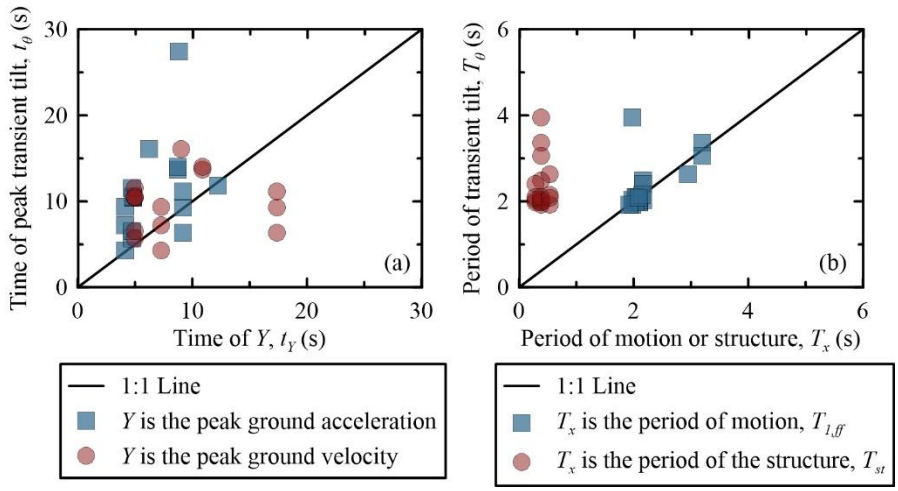

Fig. 5 – Relationships among (a) the timing of the peak transient tilt, the time of the peak ground acceleration, and time of the peak ground velocity and (b) the predominant periods of the transient tilt and the horizontal acceleration in the far field and the first period of the structure.

The results in Figures 4 and 5 support the decisions made in modeling Eqs. (2) through (10) and the recommendation to use the time history parameters of the CAV accumulation plot for the settlement and tilt time histories. These aspects of the methodology could be refined with a larger database that included more variation in the shapes of the I_A and CAV accumulation plots of the motions, the predominant periods of the motions, and the vibration periods of the structures. A larger database would also enable us to quantify the uncertainty around these relationships and propagate it forward into dynamic analysis of structures.

Figure 7 shows observed and fitted time histories for two of the centrifuge tests in [4]. The modeled settlement time histories match the observed histories well. The modeled tilt time histories do not perfectly capture each peak in the observed histories, but do fit the peak response, its timing, and the frequency content, and this conceit is necessary for the practicality of the procedure.

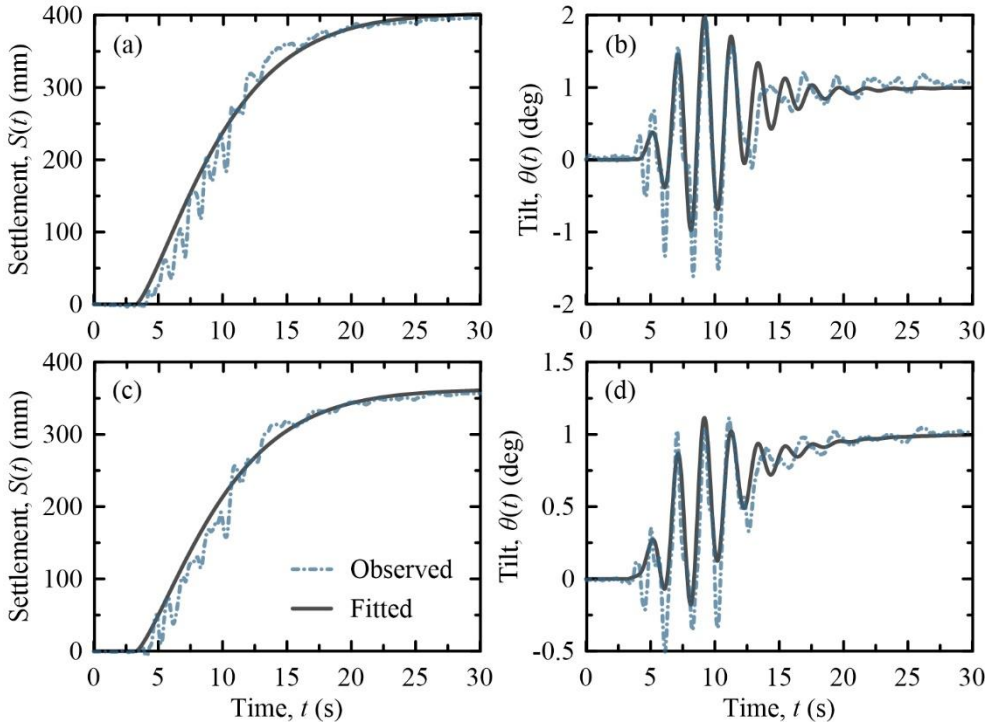

Fig. 7 – Observed and fitted time histories of settlement and tilt for centrifuge tests from [4]. The time histories in (a) and (b) correspond to a single prototype structure/profile and the time histories in (c) and (d) correspond to another prototype structure/profile.

4. Implementation and Example

This section begins with an acceleration time history, an estimate of permanent foundation settlement, and estimates of residual and peak transient tilt, and follows the process described above to generate settlement and tilt time histories. The structural model used in this example is a 1-story reinforced concrete structure from [14]. This example uses the acceleration time history shown in Figure 3, which was recorded in [4], and applies θ_r equal to 1.0 degrees and θ_{pt} equal to 1.4 degrees. The average foundation settlement applied is 50 mm. The horizontal ground motion has a PGA of 1,050 cm/s^2, a PGV of 363 cm/s, and a CAV of 2,512 cm/s.

Table 2 provides the peak and residual interstory drift ratios (IDR) in the building for the following cases: (1) a fixed-base structure with no adjustment for foundation displacement; (2) a fixed-base structure with foundation rotation and settlement applied pseudostatically after the end of shaking; and (3) a fixed-base structure with transient foundation rotation and settlement applied during shaking. The residual drift increases only slightly (from 0.27% to 0.29%) when the foundation displacement is applied pseudostatically, but

substantially (from 0.27% to 0.82%) when it is applied transiently. The peak transient drifts are also increased when the displacement is transient, and the increase is larger than the value of the peak rocking drift (i.e., θ_{pt}).

Table 2 –Results for the case study.

Output	Case 1 – No foundation displacement	Case 2 – Pseudostatic foundation displacement	Case 3 – Transient foundation displacement
Peak transient rocking drift (%)	0.00	0.00	0.02
Peak transient flexural drift (%)	1.9	1.9	2.3
Peak transient total drift (%)	1.9	1.9	2.3
Residual rocking drift (%)	0.00	0.02	0.02
Residual flexural drift (%)	0.27	0.27	0.80
Residual total drift (%)	0.27	0.29	0.82

Figure 6 shows time histories of IDR for the three cases presented in Table 2. These time histories demonstrate that the shift from Case 1 to Case 3 reflects dynamic interaction of the acceleration and the applied rocking response (i.e., these factors combine to create a large excursion by the roof at approximately 9 seconds, from which it is unable to recenter before the end of shaking).

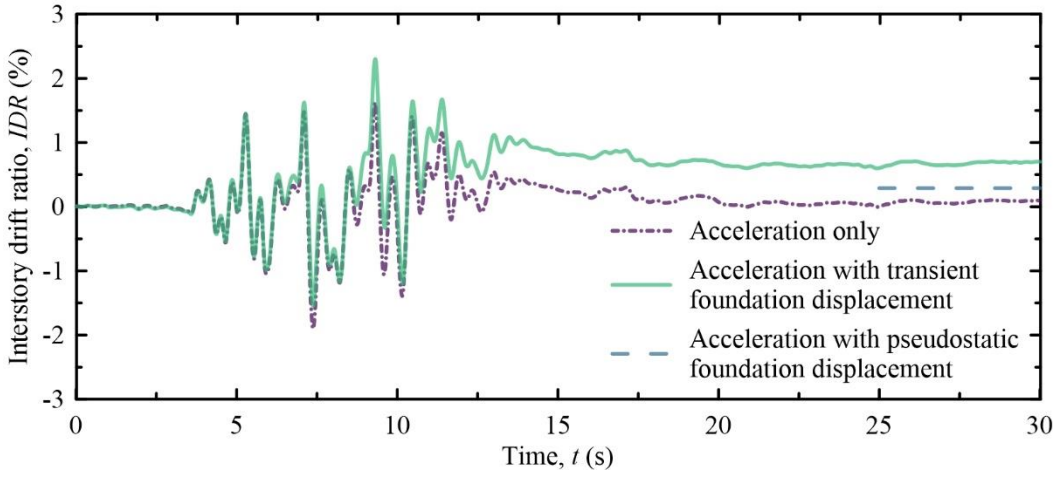

Fig. 6 – Time histories of the interstory drift ratio for the 1 story reinforced concrete structure [14] subjected to the loading regimes described in Table 2: acceleration only, acceleration with pseudostatic foundation displacement applied after shaking, and acceleration with transient foundation displacement.

5. Concluding remarks

This study presents a methodology for generating time histories of foundation displacement that correspond to a given acceleration time history and estimates of settlement (S), residual tilt (θ_r), and peak transient tilt (θ_{pt}) about the foundation. The modeling decisions involved in developing this methodology are justified using results from prior centrifuge experimentation. These modeling decisions might be improved when more results from centrifuge tests become available, particularly tests that include more variation in the time-frequency

content of ground motions and the first vibration period of the structure. More data are also needed to propagate uncertainty around the time history parameters into subsequent analysis.

This study also presents an example of the results obtained from dynamic analysis of structures using time histories generated with the proposed methodology. For this example, the incorporation of transient foundation displacement increased the peak and residual drifts of the structure substantially. The example also demonstrates that pseudostatic application of foundation displacement after a typical dynamic analysis of a structure may not fully reflect the impact of liquefaction on superstructural response. Dynamic analyses of shallow-founded structures on liquefiable ground should therefore use time histories of foundation displacements to capture the interactions between the acceleration and the applied rocking.

6. Acknowledgments

This study was partly supported by the U.S. Department of Education under award number P200A150042.

7. References

[1] Bray, J. D., Macedo, J. (2017). 6th Ishihara lecture: Simplified procedure for estimating liquefaction-induced building settlement. *Soil Dynamics and Earthquake Engineering*, **102**, 215-231.

[2] Bullock, Z., Karimi, Z., Dashti, S., Porter, K., Liel, A. B., Franke, K. W. (2018). A physics-informed semi-empirical probabilistic model for the settlement of shallow-founded structures on liquefiable ground. *Géotechnique*, **69**(5), 406-419.

[3] Bullock, Z., Dashti, S., Karimi, Z., Liel, A. B., Porter, K. A., Franke, K. W. (2018). Probabilistic models for residual and peak transient tilt of mat-founded structures on liquefiable soils. *Journal of Geotechnical and Geoenvironmental Engineering*, **145**(2), 04018108.

[4] Dashti, S., Bray, J. D., Pestana, J. M., Riemer, M. R., Wilson, D. (2010a). Centrifuge testing to evaluate and mitigate liquefaction induced building settlement mechanisms. *Journal of Geotechnical and Geonvironmental Engineering*, **136**(7), 918-929.

[5] Dashti, S., Bray, J. D., Pestana, J. M., Riemer, M. R., Wilson, D. (2010b). Mechanisms of seismically-induced settlement of buildings with shallow foundations on liquefiable soil. *Journal of Geotechnical and Geoenvironmental Engineering*, **136**(1), 151-164.

[6] Olarte, J., Paramasivam, B., Dashti, S., Liel, A. B., Zannin, J. (2017). Centrifuge modeling of mitigation-soil-foundation-structure interaction on liquefiable ground. *Soil Dynamics and Earthquake Engineering*, **97**, 304-323.

[7] Paramasivam, B., Dashti, S., Liel, A. B. (2018). Influence of prefabricated vertical drains on the seismic performance of structures founded on liquefiable soils. *Journal of Geotechnical and Geoenvironmental Engineering*, **144**(10).

[8] Cressie, N. (1985). Fitting variogram models by weighted least squares. *Journal of the International Association for Mathematical Geology*, **17**(5), 563-586.

[9] Gumbel, E. J. (1958). *Statistics of Extremes*. Columbia University Press.

[10] Husid, R., H. Median, J. Rios (1969). Analysis de Terremotos Norteamericanos y Japonsesses, in *Revista del IDIEM 8, Chile*.

[11] Arias, A. (1970). A measure of earthquake intensity, in *Seismic Design of Nuclear Power Plants*, R. J. Hansen, Editor, The Massachusetts Institute of Technology Press.

[12] Karimi, Z., Dashti, S., Bullock, Z., Porter, K., Liel, A. B. (2018). Key predictors of structure settlement on liquefiable ground: A numerical parametric study. *Soil Dynamics and Earthquake Engineering*, **113**, 286-308.

[13] Bullock, Z., Dashti, S., Liel, A. B., Porter, K. A., Karimi, Z. (2019). Assessment supporting the use of outcropping rock evolutionary intensity measures for prediction of liquefaction consequences. *Earthquake Spectra*, **35**(4), 1899-1926.

[14] Haselton, C. B., Liel, A. B., Deierlein, G. G., Dean, B. S., Chou, J. H. (2011). Seismic collapse safety of reinforced concrete buildings. I: Assessment of ductile moment frames. *Journal of Structural Engineering*, **137**(4), 481-491.